BioBacta

Journal of Bioscience and Applied Research

www.jbaar.org

Biochemical and pathological evaluation of the effectiveness of nano-targeted sono-photodynamic therapy in breast cancer

Ahmed A Jasim[1,2], Jubran M. Abdulrahman[1,3] , Samir A. Abd El-kareem[4], Gihan Hosny[1]*

[1]Institute of Graduate Studies & Research, Alexandria University, Egypt.

[2]Al-NahrainUniversity, Biotechnology Research center, Baghdad, Iraq.

[3]Center of Research and Educational Studies, Ministry of Education, Baghdad, Iraq.

[4]Medical Research Institute, Alexandria University, Egypt.

* To whom correspondence should be addressed:
Email: gihan1hosny@gmail.com; Tel: (+203) 4295007; Fax: (+203) 4285792.

Abstract

Background: Sono-photodynamic therapy (SPDT) is a novel cancer treatment therapy that uses the light of a particular wavelength and sound of a particular frequency to activate a light- and sonosensitive material which attaches selectively tumor cells, causing their breakdown. The present work aims to investigate biochemically and pathologically the effectiveness of using SPDT in combination with either nano-5-aminolevulinic acid (nano-ALA) or nano-Chlorophyll (nano-Chl), as sono-photosensitizers, in curing Ehrlich ascites carcinoma tumor implanted to group of mice. **Methods:** A total of 130 male Swiss albino mice with age 60–65 day, weighing 20 ± 2.0 g, were used in this experiment. Two sources of energy were used; namely infrared laser (IR) and Ultrasound for 3 min. When the tumor had grown to about 10 mm in diameter at day 10 after inoculation, the treatment strategy was started. Six experimental groups were investigated. Biochemical analyses were carried out to detect the serum levels for activities of oxidative stress enzymes, liver and kidney functions. Pathological analyses were carried out to evaluate the effect of different treatment modalities on tumor treatment. **Results:** It was observed that SPDT utilizing nano-ALA or nano-Chl ameliorated the activity levels of the studied enzymes in mice bearing tumor lesions, indicating the safe and non-toxic treatment modality. Pathological evaluation showed that targeted SPDT caused almost complete destruction of cancer cells. **Conclusion:** The results suggest that nano-ALA or nano-Chl could be used as novel and safe nano-materials with great potential as effective drug delivery system in cancer-targeted SPDT.

Key words: Sono-dynamic therapy (SDT), photo-dynamic therapy (PDT), Sono-photodynamic therapy (SPDT), nano-chlorophyll, nano-5-aminolevulinic acid, Cancer treatment.

Introduction

SPDT is available as an effective treatment for cancer in England, Mexico, Israel, China and Cape Town. It has been shown to be efficient for deep-seated tumors such as bowel and ovarian cancer, as well as metastatic cancer, in particular when spread to bone, lung and liver tissues [(1)] . The vast majority of patients with advanced cancer treated with SPDT live longer than predicted and in 75% of cases, there is significant tumor cell destruction.[(2)] At the beginning of the treatment, patients consume or are intravenously given a nanomaterial-based light-sensitive compound which binds selectively to tumor cells. It stays absorbed by cancer cells but is quickly released by healthy cells. The active agent is absorbed into the body 48-72 h prior to treatment and intravenous ozone is administered just before the treatment to enhance its effects; ozone, which is a super-oxygen compound, inhibits cancer cell growth, as cancer cells are more active under low oxygen thresholds [(3-6)] . The patient is then placed in a specialized light bed and exposed to thousands of light emitting diodes (LED) which emit red and infrared light waves, followed by ultrasound treatment at a definite frequency in tumor localized areas of the body. The excited sensitizer stimulates the formation of reactive oxygen species (ROS) from the molecular oxygen present in the cells. ROS lead the cancer cells to die by severely increasing the level of oxidative stress, causing genetic and cell membrane damage. The death of cancer cells activates the immune system that responds to the call to clean-up the debris and attacks the remaining malignant cells that are finally recognized as invaders. SPDT also blocks angiogenesis, the crucial conduit for cancer cell nutrition. Since the whole body is exposed to the light, all cancer or pre-cancerous cells within a range are affected, allowing the destruction and inhibition of cancer anywhere in the body [(7-9)] . This treatment is entirely safe and the only side-effects are related to the destruction of the tumor cells that produce an inflammatory response intended at clearing the dead tumor tissue [(6)] .

The liver is the organ involved in the biotransformation of drugs and other hepato-toxicants. The serum level of bilirubin and activities of liver enzymes; ALT, AST, ALP, and GGT, are considered reliable indices of hepatotoxicity [(10,11)] . Increase in serum ALT and AST may have resulted from leakage from damaged hepatocytes (hepatocellular injury) [(12)] . The serum level of bilirubin also indicates hepatotoxicity. Bilirubin is found in the liver, bile, intestines, and the reticulo-endothelial cells of the spleen while ALP and GGT are associated with the cell membrane [(13)]. Serum bilirubin and activities of ALP and GGT are found to increase in conditions associated with hepatobiliary injury (decrease in hepatic clearance of bilirubin) and overproduction or leakage of ALP and GGT [(14)]. Creatinine and urea are metabolic products which are removed from circulation by the kidney to prevent their accumulation. Increase in serum level of these substances is regarded as an indication of loss of renal function [(15-18)]. The underlying work was conducted aiming at investigating the biochemical and pathological effects of using SPDT in combination with sono-photosensitizer (nano-ALA or nano-Chl) loaded on graphene oxide nanoparticles as an up-to-date treating cancer modality for the purpose of curing Ehrlich ascites carcinoma, EAC.

Materials and Methods

Synthesis of nano-material

In the present work nanographene oxide (NGO) was prepared using nature graphite powders as the raw materials by a modified Hummers method [(18)]. Also conjugation of folic acid with graphene oxide (FA-NGO) was used. Folic acid (FA) molecules were conjugated to the NGO as described by Jonsson et al [(19)]. Sonophotosensitizer was loaded by FA-NGO (FA-GO-CHL). 5-aminolevulinic acid or Chlorophyll (purchased from Molbase Chemicals Co. China) was used as sonophotosensitizer; chemically active by absorption of light and/or ultrasound. The loading efficiency of sonophotosensitizer was calculated according to UV absorbance at 663 nm. Every

experiment was repeated for three times. Nano-sonophotosensitizer was administered by intraperitoneal (IP) injection to tumor-bearing mice for 15 days 18-20 hours before exposure to either photo and/or sonodynamic treatment modality.

Animal treatment

A total of 130 male Swiss albino mice with age 60-65 day, weighing 20 ± 2.0 g, were purchased from National Cancer Institute, Cairo University, were induced Ehrlich Tumor Cells. Ehrlich ascites carcinoma tumor cells, 2 x 10^6 mammary in origin, diluted approximately (1-9) in 0.9 % saline were inoculated subcutaneously on the left side of mice. The animals were housed in plastic cages and were kept under natural light with diet and water available. When the tumor had grown to about 10 mm in diameter at day 10 after inoculation, the treatment protocol was started. Use of experimental animals in the study protocol was carried out in accordance with the ethical guidelines of the Medical Research Institute, Alexandria University (Guiding Principles for Biomedical Research Involving Animals, 2011).

The experimental animal treatment groups were as follows:

Group I: (30 mice)

a) **10 mice:** Control without tumor.

b) **10 mice:** Tumor bearing mice without treatment.

c) **10 mice:** Tumor bearing mice treated with (FA-NGO-CHL) only.

Group II: (20 mice, laser irradiated group)

a) **10 mice:** were exposed to Infra-Red Laser (4000 Hz) for 3 minutes.

b) **10 mice:** were exposed to Infra-Red Laser (7000 Hz) for 3 minutes.

Group III: (20 mice, ultrasound group)

a) **10 mice:** were exposed to pulsed ultrasound for 3 minutes.

b) **10 mice:** were exposed to continuous ultrasound for 3 minutes.

Group IV: (20 mice, (FA-NGO- CHL), laser group)

The mice of this group were injected intraperitoneally (IP) with (FA-NGO- CHL), then the tumor site will be irradiated to laser light at same conditions of group II.

Group V: (20 mice, (FA-NGO- CHL), ultrasound group)

The mice of this group were injected (IP) with (FA-NGO- CHL), then were divided into 2 sub-groups. The tumor site was irradiated to ultrasound at same conditions of group III.

Group VI: (20 mice, combined treatment groups)

a) **10 mice:** The tumor site was irradiated to laser light (7000 Hz) for 3 minutes, followed by pulsed ultrasound for 3 minutes.

b) **10 mice:** Injected (IP) with (FA-NGO- CHL). The tumor sites were irradiated to laser light (7000 Hz) for 3 min, followed by pulsed ultrasound for 3 minutes.

For laser and ultrasound exposure, the mice were anesthetized with diethyl ether. The hair over the tumors was shaved off. The mice were fixed on a board with the tumor upwards. For laser exposure, the probe was placed nearly on the tumor, which was irradiated with laser for three minute at the different conditions as mentioned before. After PDT, animals were maintained in the dark to avoid skin irritation. Exposure of mice tumor to the laser beam was carried out using an Infrared diode laser, model LAS 50- Hi-Tech Fysiomed, Germany operated at a wavelength of 904 nm and a peak power of 50 W at a frequency up to 7000 Hz.

For the ultrasound exposure, gel was added locally and the probe was placed nearly on the tumor, which was irradiated with ultrasound for three minutes at the different conditions as mentioned before. Exposure of

Ehrlich Tumor was carried out using an ultrasonic therapy instrument (Model CSl Shanghai, No. 822 Factory. China). This instrument, uses electronic tube to generate an electric oscillation with frequency 0.8 MHz and power output which converted to ultrasonic mechanical energy by means of ultrasonic transducer (calcium zirconate -titanate). The mechanical ultrasonic energy has a beam power density which can be adjusted from 0.5 to 3W/cm^2. Sonocation time can be adjusted up to 30 minutes, while the set-time is over, the power supply cut off automatically and intermittent alarming sound may be given. This instrument operates at both continuous and pulsed modes (pulse frequency 1000 Hz, duty ratio 1/3 and average power density from 0.15-1 W/cm^2).

Biochemical Examination

All biochemical analyses were done on Indiko Plus Auto-analyzer, with a capacity of up to 350 photometric tests/ hour.

1. Antioxidant activity

i. **Estimation of Malondialdehyde (MDA)**
Lipid Peroxidation (MDA) was performed as described by manufacturer using assay kit of Biovision (Catalog # K739-100).

ii. **Estimation of Total Antioxidant Capacity (TAC)**
Total Antioxidant Capacity (TAC) was performed as described by manufacturer using assay kit of Biovision (Catalog #K274-100).

iii. **Estimation of Glutathione Reductase Activity (GR)**
Glutathione Reductase Activity was performed as described by manufacturer using assay kit of Biovision (Catalog #K761-100).

iv. **Estimation of Glutathione-S-Transferase Activity (GST)**
GST Colorimetric Activity was performed as described by manufacturer using assay kit of Biovision (Catalog #K263-100).

v. **Estimation of Superoxide Dismutase Activity (SOD)**
Superoxide Dismutase Activity (SOD) was performed as described by manufacturer using assay kit of Biovision (Catalog #K335-100).

vi. **Estimation of Catalase Activity (CAT)**
Catalase Activity Colorimetric was performed as described by manufacturer using assay kit of Biovision (Catalog #K773-100).

2. Kidney Function Test

I. Determination of blood urea (urease-colorimeteric method)

Principle

The reaction involved in the assay system is that urea is hydrolyzed in the presence of water and urease to produce ammonia and carbon dioxide.

$$\text{Urea} + H_2O \xrightarrow{\text{urease}} 2\,NH_3 + CO_2$$

The free ammonia in an alkaline pH and in the presence of indicator forms colored complex proportional to the urea concentration in the specimen.

II. Determination of Creatinine

It was performed as described by Jaffe's Method, using Creatinine standard (2.0 mg/dl), picric acid (14 mmol/l) and sodium hydroxide (250 mmol/l).

3. Liver Function Test

I. ALT (GPT) Colorimetric test

It was performed as described in Reitman and Frankel method; briefly:

$$\text{L- Alanine} + 2\ \text{Oxaglutarate} \xrightarrow{\text{ALT/GPT}} \text{Pyruvate} + \text{Glutamate}$$

ALT/GPT is measured by monitoring the concentration of pyruvate hydrazone formed with 2, 4 dinitrophenyl-hydrazine (color reagent; 1 mmol/L).

II. AST (GOT)

It is determined by reagent IFCC method 2 part liquid; its principal is:

L- Aspatate + 2- oxoglutarate $\xrightarrow[\text{MDH}]{\text{AST}}$ Oxalacetate + Glutamate

Oxaloacete + NADH $\xrightarrow[\text{LDH}]{}$ L- Malate + NAD

Sample Pyruvate + NADH ⟶ L- Lacate + NAD

III. Gamma-Glutamyltransferase (GGT)

Principle

The GGT- 2 part liquid method utilizes Glucana in the following reaction, which is initiated by the addition of sample. GGT present in the sample catalyzes the transfer of the glutamyl group from the substrate to glycylglycine forming glutamylglycylglycine and 5-amino-2-nitrobenzoate.

L- γ -glutamyl-3-carboxy-4-nitroanilide + glycylglycine

↓ GGT

L- γ-glutamylglycylglycine + 5-amino-2-nitrobenzoate

The rate of formation of 5-amino-2-nitrobenzoate is proportional to the activity of GGT present in the sample and can be measured kinetically at 405nm.

Histopathological Examination

Small pieces of Ehrlich Tumor cells of the experimental groups were processed and examined by Hematoxylin and Eosin (H&E) method as follows:

1. The small pieces of Ehrlich Tumor cells were fixed at 10% formaldehyde.
2. Then dehydrated in ascending grades using alcohol.
3. Embedded in paraffin to produce paraffin block.
4. The blocks were cut into 3-4 µm thick sections and floated in water bath.
5. Cleaned with xylene, then rehydrated in descending grades of alcohol.
6. Stained with Haematoxlin and Eosin stain.
7. Cleaned again ethylene.
8. Covered by covering slides, thus the slides were prepared to be examined by light microscopy.

Statistical analysis

Analysis of numeric data was performed using one-way ANOVA; it is a parametric statistical test that used to compare the means for certain data of more than two independent groups which follow a normal distribution. The given graphs were constructed using Microsoft excel software. All statistical analysis were done using two tailed tests and alpha error of 0.05. P value less than or equal to 0.05 was considered to be statistically significant.

Results

Antioxidant activities

In the underlying study, the increase in lipid peroxidation was reported in control group which carried EAC. In all the irradiated groups and that irradiated and treated without N5-ALA, a significant increase in the levels of MDA was observed. Animals in groups irradiated with IRL or US or both with nano-5-ALA exhibited significantly low levels of MDA, as compared with the cancer control group or with treated mice without activation of N5-ALA, as illustrated in Table 1. ANOVA test revealed statistical significant differences between groups at $p \leq 0.05$ (comparable results were obtained using nano-Chl).

The implanted mice with EAC showed decreased activities of antioxidants (SOD, CAT, GR, GST and TAC) in comparison with normal animals. On the other hand, there was a significant increase in the enzymatic and non-enzymatic antioxidant guard in the groups irradiated with IRL or US or both with nano-5-ALA when compared with cancer control group or with treated mice without activation of nano-5-ALA, as illustrated in Table 1. and Figures 3.8 to 3.13. ANOVA test revealed statistical significant differences between groups at $p \leq 0.05$ (comparable results were obtained using nano-Chl).

The results of examination of antioxidant activities indicate the effectiveness and safe use of nano-5-ALA or nano-Chl-targeted sono-photodynamic therapy in ameliorating enzyme activities to almost their normal levels with subsequent cancer treatment.

Table 1. Activities of antioxidant enzymes in the different studied groups.

Group Name	GST (U/ml)	GR (mU/ml)	CAT (mU/ml)	TAC (mM/L)	SOD (U/ml)	MDA (nmol/ml)
Normal	3.95± 0.92	0.082 ± 0.01	814.26 ± 3.66	0.73 ± 0.01	1771.5± 5.32	24 ± 0.05
EAC	0.39 [a] ± 0.1	0.015 [a] ± 0.01	92.82 [a] ± 0.54	0.02 [a] ± 0.01	37.48 [a] ± 0.34	251.12 [a] ± 1.58
N5-ALA	0.40 [a] ± 0.15	0.016 [a] ± 0.01	93.1 [ab] ± 0.75	0.03 [ab] ± 0.01	38.2 [ab] ± 1.58	250.3 [ab] ± 1.47
4000 IRL	0.53 [abc] ± 0.21	0.022 [bc] ± 0.01	125.04 [abc] ± 1.25	0.12 [abc] ± 0.01	155.54 [abc] ± 1.33	195.12 [abc] ± 0.06
7000 IRL	0.57 [abc] ± 0.16	0.025 [abc] ± 0.01	242.73 [abc] ± 0.74	0.25 [abc] ± 0.01	202.4 [abc] ± 1.35	171.55 [abc] ± 0.05
4000 IRL +N5-ALA	0.59 [abc] ± 0.18	0.026 [bc] ± 0.01	243.3 [abc] ± 2.74	0.26 [abc] ± 0.01	210 [abc] ± 2.07	161.3 [abc] ± 0.40
7000 IRL +N5-ALA	0.7 [abc] ± 0.15	0.031 [abc] ± 0.01	253.4 [ab] ± 2.40	0.31 [abc] ± 0.01	281.16 [abc] ± 0.16	145.62 [abc] ± 0.34
Cont. US	1.11 [abc] ± 0.12	0.036 [abc] ± 0.01	276.35 [abc] ± 2.81	0.36 [abc] ± 0.01	375 [abc] ± 1.16	132.55 [abc] ± 1.04
Puls. US	1.32 [abc] ± 0.13	0.037 [abc] ± 0.01	361.52 [abc] ± 5.54	0.37 [abc] ± 0.01	375.68 [abc] ± 0.33	124.11 [abc] ± 1.58
Cont.US +N5-ALA	1.5 [abc] ± 0.1	0.038 [bc] ± 0.01	390.3 [abc] ± 3.73	0.38 [abc] ± 0.01	602 [abc] ± 1.92	108.44 [abc] ± 0.92
Pulsed US +N5-ALA	2.4 [abc] ± 0.5	0.043 [abc] ± 0.01	510.1 [abc] ± 3.99	0.46 [abc] ± 0.01	811 [abc] ± 1.90	104.7 [abc] ± 0.95
7000 IRl+ US						
Pulsed	3.22 [abc] ± 0.2	0.048 [abc] ± 0.01	530.8 [abc] ± 4.01	0.52 [abc] ± 0.01	1490 [abc] ± 1.58	84.3 [abc] ± 0.05
Puls. +N5-ALA	3.3 [abc] ± 0.3	0.049 [abc] ± 0.01	631.5 [abc] ± 3.70	0.53 [abc] ± 0.01	1512 [abc] ± 1.50	48.2 [abc] ± 0.58
F	43.097	9.415	1463	124.9	27230	1732
P	<0.001*	<0.001*	<0.001*	<0.001*	<0.001*	<0.001*

F: F value for ANOVA test
a: Significant with Normal group
b: Significant with EAC group
c: Significant with N5-ALA group
*: Statistically significant at $p \leq 0.05$
Data was expressed by using mean ± SD.

Liver and kidney functions

The biomarkers of renal function, namely; creatinine and urea, were estimated. The EAC caused a significant increase in the serum urea and creatinine levels in the studied groups. On the other hand the nano-5-ALA caused decrease in the levels of serum creatinine and urea which is probably an indication of renal protection, as shown in Table 2. This also confirms the protective role of nano-5-ALA against renal toxicity. ANOVA test revealed statistical significant differences between groups at $p \leq 0.05$ (comparable results were obtained using nano-Chl).

Also the biomarkers of hepatic function, ALT, AST and GGT, were estimated. The EAC caused a significant increase in the serum activities of ALT, AST and GGT of the tumor treated groups. However, in the EAC treated groups with nano-5-ALA a decrease in serum levels of ALT, AST, and GGT, were observed which is an indication of the hepatoprotection by N5-ALA, i.e., this confirms the protective role of nano-5-ALA against hepatotoxicity, as shown in Table 2. ANOVA test revealed statistical significant differences between groups at $p \leq 0.05$ (comparable results were obtained using nano-Chl).

The results of examination of liver and kidney functions indicate the effectiveness and safe use of nano-5-ALA or nano-Chl-targeted sono-photodynamic therapy in ameliorating toxicity on liver and kidneys with subsequent cancer treatment.

Table 2. Renal and hepatic functions in the different studied groups

Group Name	Urea (mg/dl)	Creatinine (mg/dl)	ALT (U/l)	AST (U/l)	GGT (U/l)
Control	11.1 ± 0.69	0.22 ± 0.08	39 ± 1.08	35.94 ± 0.28	1.3 ± 0.41
EAC	30.6 ± 0.49	0.62 ± 0.07	204 [a] ± 3.69	331.06 [a] ± 0.98	2.8 ± 0.39
N5-ALA	30.5 ± 0.95	0.61 ± 0.05	200 [ab] ± 2.87	326.6 [ab] ± 0.62	2.76 ± 0.45
4000 IRL	28.2 ± 0.50	0.5 [c] ± 0.06	156 [bc] ± 1.59	210.28 [abc] ± 0.1	2.5 ± 0.2
7000 IRL	24.2 ± 0.32	0.44 ± 0.18	131 [abc] ± 0.77	150.78 [abc] ± 0.6	2.4 ± 0.44
4000 IRL +N5-ALA	23.9 ± 0.66	0.4 ± 0.03	113.4 [bc] ± 0.66	148.4 [ab] ± 0.02	2.38 ± 0.43
7000 IRL +N5-ALA	22.5 ± 0.57	0.39 ± 0.01	93.8 [bc] ± 0.59	129.3 [bc] ± 0.50	2.2 ± 0.41
Cont. US	21.4 ± 0.43	0.34 ± 0.18	84.2 [abc] ± 0.34	59.4 [abc] ± 0.60	2.01 ± 0.42
Puls. US	21.2 ± 0.84	0.33 ± 0.04	74 [bc] ± 0.16	55.4 [bc] ± 0.99	1. 9 ± 0.37
Cont. US +N5-ALA	20.1 ± 0.78	0.32 ± 0.02	68.1 [bc] ± 0.24	51.3 [bc] ± 0.43	1.88 ± 0.22
Puls. US +N5-ALA	19.9 ± 0.59	0.30 ± 0.09	63.9 [bc] ± 0.06	49.1 [bc] ± 0.88	1.7 ± 0.47
7000 IRl+ US					
Pulsed	18 ± 0.50	0.25 ± 0.08	55.2 [abc] ± 0.69	44.92 [bc] ± 0.99	1.55 ± 0.39
Puls. +N5-ALA	17.5 ± 0.65	0.24 ± 0.01	53.8 ± 0.61	41.3 [bc] ± 0.41	1.51 ± 0.46
F	220.762	6.689	419.8	7889	4.424
P	<0.001*	<0.001*	<0.001*	<0.001*	<0.001*

F: F value for ANOVA test
a: Significant with Normal group
b: Significant with Only EAC group
c: Significant with D1 only group
*: Statistically significant at $p \leq 0.05$
Data was expressed by using mean ± SD.

Histopathological examination

Figures 1 to 3 show the histopathological examination for tumor tissue of all studied mice groups. Comparable results were obtained for nano-Chl or nano-5-ALA, as sono-photosensitizers. The histopathological evaluation revealed that all tumors from the group of tumor bearing mice (as a control group) without treatment were highly malignant cells and the tumors showed 5-10% necrosis (Figure 1). Group of tumor bearing mice treated with nano-Chl or nano-5-ALA showed 10-14% necrosis due to nano-Chl or nano-5-ALA inactivation. Group of mice treated with IRL; 4000Hz or 7000Hz, showed significant areas of necrosis from 40 to 55% (Figure 1c&d).

In the group of mice injected IP with nano-Chl or nano-5-ALA then the tumor site were irradiated to 4000Hz or 7000Hz showed significant areas of necrosis ranged from 65 to 75% (Figures 2). Group of mice treated with pulsed or continuous ultrasound at power density of 3W/cm^2 for 3 minutes showed significant areas of necrosis ranged from 55 to 60%.

The Group of mice injected IP with nano-Chl or nano-5-ALA, then the tumor site was irradiated to pulsed or continuous ultrasound the areas of necrosis ranged from 74 to 79%, when compared with only EAC group (Figure 3).

While in case of combination groups, 4000Hz or 7000Hz followed by pulsed ultrasound in groups of mice injected IP with nano-Chl or nano-5-ALA, Large foci of necrosis areas from 80 to 95% were present which were distinctly appeared (Figure 3).

The results of histopathological examination indicate the effectiveness of nano-5-ALA or nano-Chl-targeted sono-photodynamic therapy in destruction and necrosis of cancer cells with subsequent success in cancer treatment.

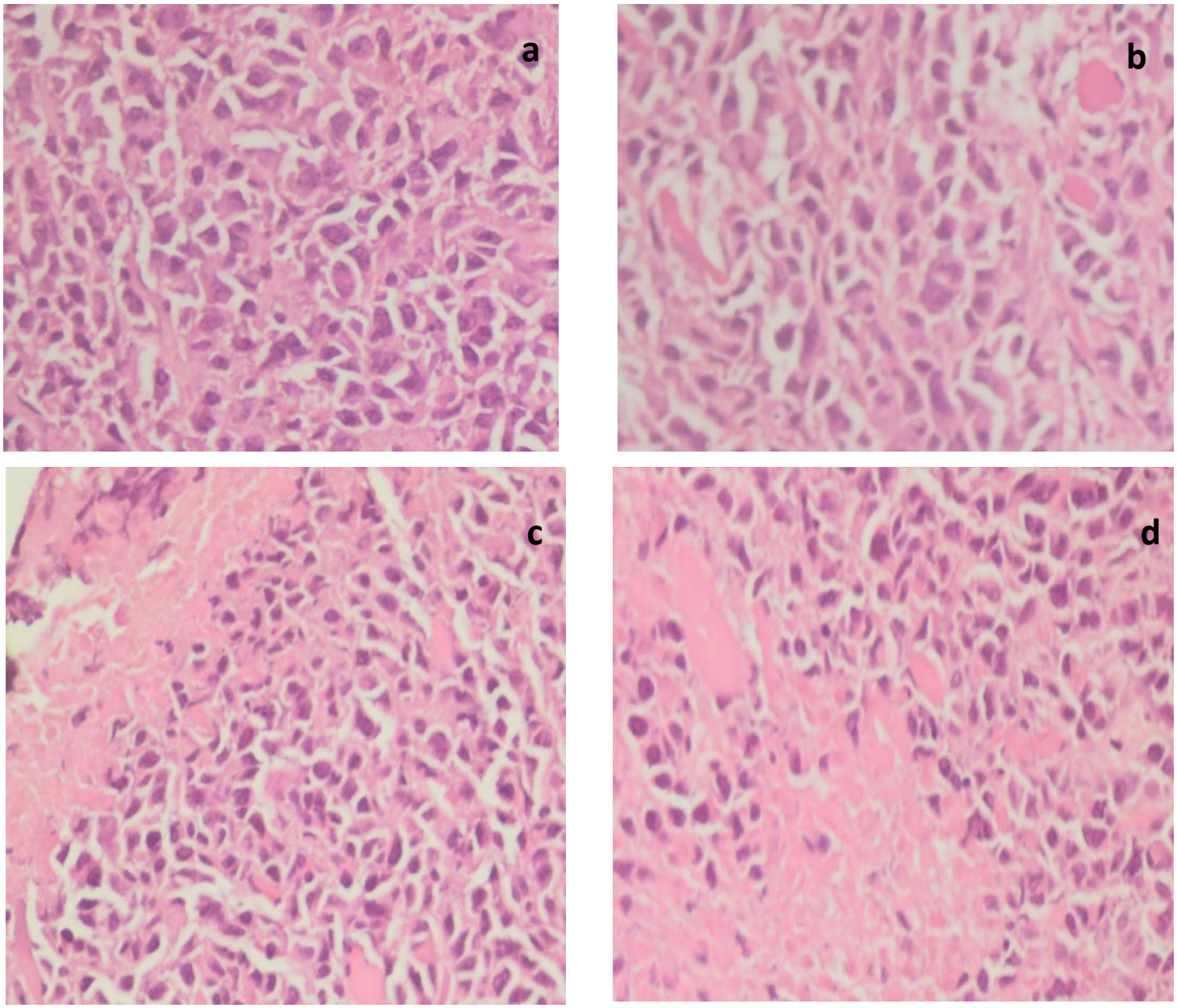

Figure 1. Histopathology of different studied groups (H&E ×400); a, Group of tumor bearing mice without treatment as a control group: [poorly differentiated carcinoma (necrosis; 0-5%)]; b, Group of tumor bearing mice treated with nano-Chl as sono-photo-sensitizer only: [poorly differentiated carcinoma (necrosis;10-14%)]; c, Group of mice treated with 4000 Hz Infra-Red Laser (IRL) for 3minutes (H&E×400): [poorly differentiated carcinoma (necrosis;40%)]; and d, Group of mice treated with IRL group, 7000Hz, for 3 minutes (H&E×400): [Poorly differentiated carcinoma (necrosis; 55%)].

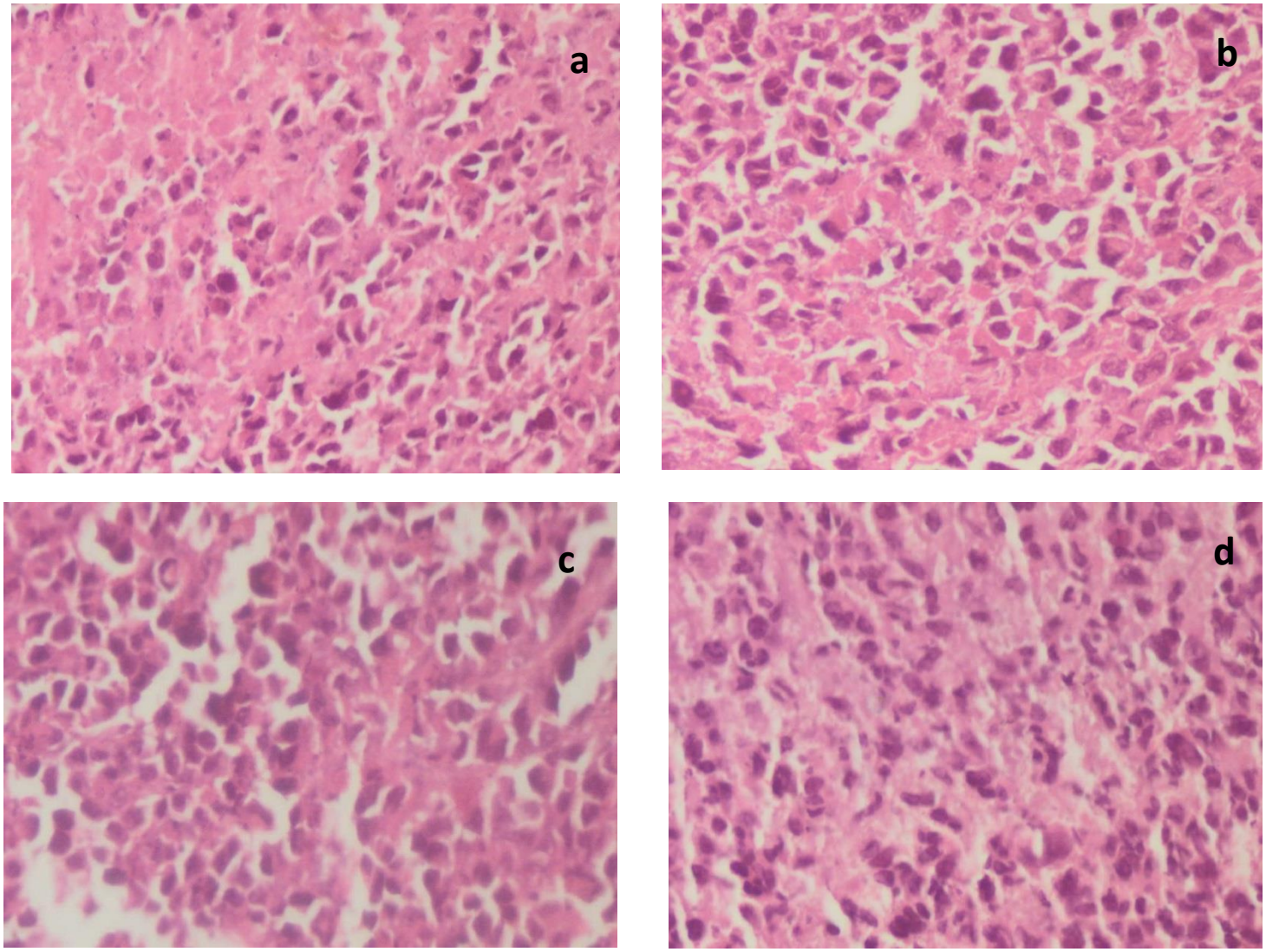

Figure 2. Histopathology of different studied groups (H&E ×400); a, Group of mice injected IP with nano-Chl, then the tumor site were irradiated to 4000 Hz IRL: [poorly differentiated carcinoma (necrosis; 65%)]; b, Group of mice injected IP with (nano-Chl), then the tumor site were irradiated to 7000 Hz IRL: [poorly differentiated carcinoma (necrosis; 75%)]; c, Group of mice treated with pulsed ultrasound at power density of 3W/cm^2 for 3 minutes: [poorly differentiated carcinoma (necrosis; 55%)]; d, Group of mice treated with continuous ultrasound at power density of 3W/cm^2 for 3 minutes: [poorly differentiated carcinoma (necrosis; 60%)].

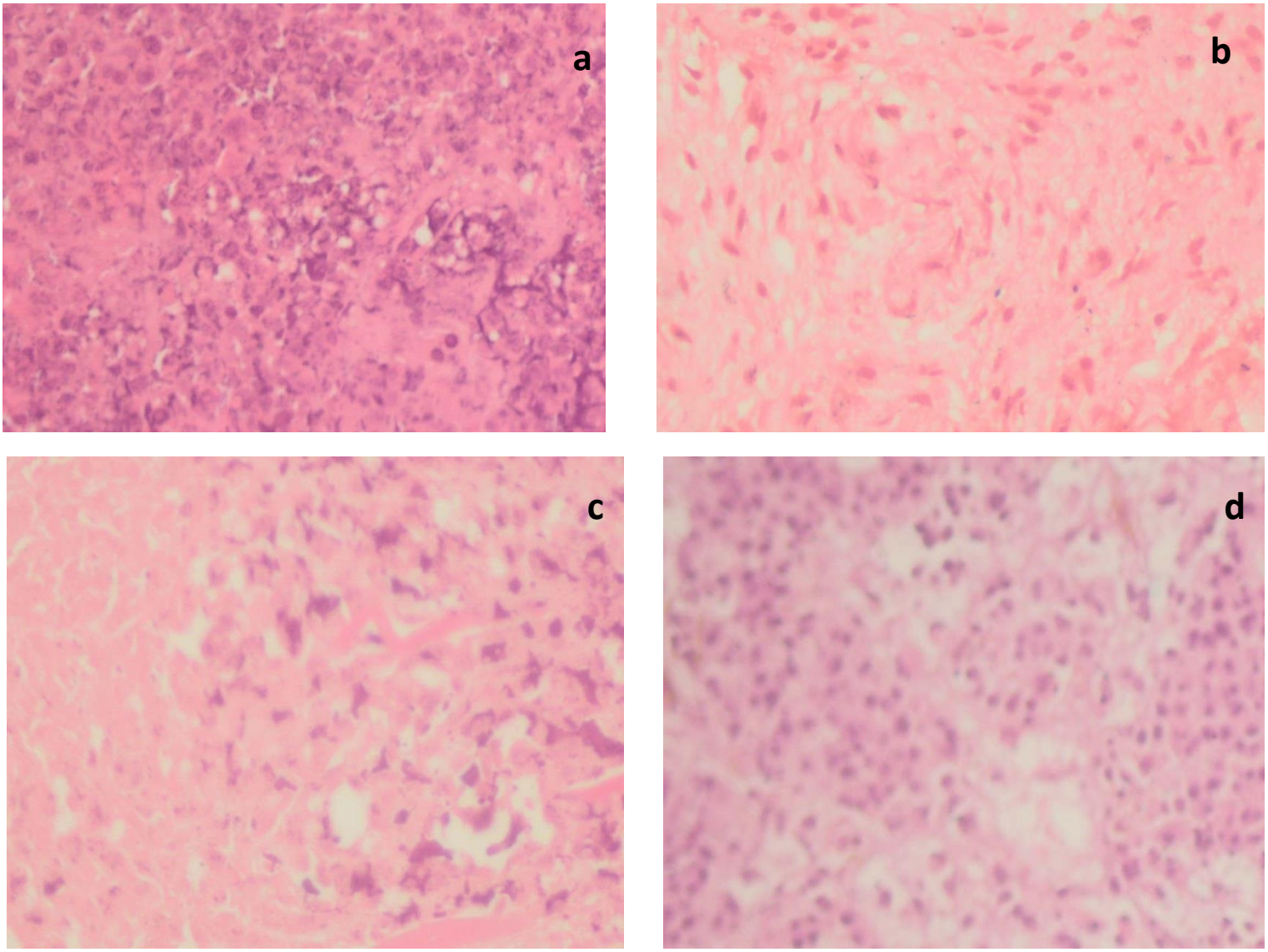

Figure 3. Histopathology of different studied groups (H&E ×400); a, Group of mice injected IP with nano-Chl, then the tumor site was irradiated to pulsed ultrasound: [poorly differentiated carcinoma (necrosis; 74%)]; b, Group of mice injected IP with (nano-Chl), followed by tumor site irradiation with continuous ultrasound: [poorly differentiated carcinoma (necrosis; 79%)]; c, Group of mice irradiated to 4000Hz IRL for 3 minutes, followed by pulsed ultrasound 3W for 3 minutes: [poorly differentiated carcinoma (necrosis; 80%)]; and d, Group of mice injected IP with (NChl). The tumor site was irradiated to 7000Hz IRL for 3 min, followed by pulsed ultrasound 3W for 3 minutes: [poorly differentiated carcinoma (necrosis; 95%)].

Discussion

A combined treatment of photosensitizer, IR laser photodynamic therapy and sonodynamic therapy were employed for the purpose to investigate whether IR laser, ultrasound each alone or combined together with nano-Chl or nano-5-ALA, as photosensitizer, could be safely administered and provide an increased local tumor cytotoxic response. Biochemical and pathological evaluation of different treatment was performed. Results revealed that nano-Chl or nano-5-ALA are potential photosensitizer and sonosensitizer for photodynamic or sonodynamic treatment of Ehrlich ascites tumor tissue. Sono-photosensitizer can play important roles in inhibiting tumor growth and even inducing cell death, which might be attributed to photo or sono-chemical activation mechanism. Infra-red laser in combination with ultrasound in the presence of nano-Chl or nano-5-ALA showed a potential antitumor effect. Sonocation followed by light photon irradiation proved their excellent efficiency as an anticancer therapy. The targeted treatment ameliorated the antioxidant activity together with liver and kidney functions, and increased necrosis of tumor cells.

MDA is used as a marker of oxidative stress, which indicates a growing interest in studying the role played by lipid peroxidation in cancer progression. MDA is low molecular weight aldehyde that can be produced from free radical attack on polyunsaturated fatty acids [(20)]. The probable reason for the elevated level of serum lipid peroxide in breast carcinoma may be due to defective antioxidant system which leads to the accumulation of lipid peroxides in cancer tissue followed by release into the blood stream. MDA constitutes a highly cytotoxic major aldehyde final peroxyl radical product of lipid peroxidation. It was claimed to be an inhibitor to protective enzymes. Hence, it could have both mutagenic and carcinogenic effects [(20)].

In the current study, all groups injected with EAC, have a significant increase in the levels of MDA as compared to the control group animals. The inhibition of peroxidation, by nano-Chl or nano-5-ALA, is mainly attributed to the scavenging of the reactive free radicals involved in the peroxidation [(20,21)]. This verifies the anti-lipid peroxidative role of nano-Chl or nano-5-ALA via their ability to scavenge free radical generation.

For the purpose of preventing cellular damage induced by ROS, there is a lot of antioxidative defense system. The anti-oxidative defense system may scavenge ROS that play an important role in the initiation of lipid peroxidation and, therefore, play a protective role in cancer development. This defense system operates through enzymatic (including SOD, GPx, GST and CAT), and non-enzymatic components (mainly GSH) [(22,23)]. SOD is the primary step of defense mechanism in the antioxidant system against the oxidative stress, as it dismutase the highly toxic superoxide anions (O^{2-}) to O_2 and H_2O_2. Gpx and catalase can scavenge H_2O_2 and convert it into harmless byproducts, thereby providing protection against ROS [(20-26)].

Also, GPx has a high potency in scavenging reactive free radicals in response to oxidative stress and detoxifies peroxides and hydroperoxides that lead to the oxidation of GSH [(22)]. Furthermore, GST catalyzes the conjugation of the thiol functional groups of GSH to electrophilic xenobiotics, leading to elimination or conversion of xenobiotic-GSH conjugate. In such reaction, the GSH is oxidized into GSSG, which can be reduced to GSH by GR with the consumption of NADPH. GSH is the most important non-enzyme antioxidant in mammalian cells. GSH is said to be involved in many cellular processes including the detoxification of endogenous and exogenous compounds and efficiently protects cells against deleterious effects of oxidative stress by scavenging free radicals, removing H_2O_2, and suppressing lipid peroxidation [(22,23)].

In the present study, the EAC bearing mice showed decreased activities of antioxidants (SOD, CAT, GR, GST and TAC) in comparison with control animals. The present data are consistent with previous findings

[24-26]. It was reported that such subsequent decrease in the antioxidant defense is due to the decreased expression of these antioxidants during mammary gland damage [26]. On the other hand, there is a significant increase in the enzymatic and non-enzymatic antioxidant guard in the animals which carried the EAC when treated with nano-Chl or nano-5-ALA, US and /or IRL when compared to the control group. This increase is due to the ability of sono-photosensitizer to prevent the formation of free radicals, enhance the endogenous antioxidant activity beyond its free radical scavenging property and the reduction of EAC lipoperoxide formation [26].

The increase in the activities of the antioxidant enzymes in nano-Chl or nano-5-ALA treated mice compared to control group indicates its effect. In this study, a statistically significant negative correlation between plasma mean levels of MDA and antioxidant activities was observed. The high MDA level could be explained by defect in the antioxidant system with accumulation of lipid peroxides in the tumor [24]. Furthermore, Sener *et al.*[20] reported statistically significant lower total antioxidant capacity with significantly higher serum MDA levels in EAC group compared to control group.

Creatinine and urea are metabolic products which are removed from circulation by the kidney to prevent their accumulation. Increase in serum level of these substances is regarded as an indication of loss of renal function. Data from this study suggest that mice groups implanted with EAC caused a loss of renal function compared with normal mice group and this is consistent with previous reports [15-18]. The biomarkers of renal function, creatinine and urea, were considered in this study. It was observed in the current study that nano-Chl or nano-5-ALA ameliorated the levels of serum creatinine and urea which is an indication of renal protection. This also confirms the protective role of nano-Chl or nano-5-ALA against mice groups implanted with EAC which induced renal dysfunction.

The liver is an organ involved in the biotransformation of drugs and other hepato-toxicants. The serum level of bilirubin and activities of the liver enzymes, ALT, AST, ALP, and GGT, are considered reliable indices of hepatotoxicity. Increase in serum ALT and AST may have resulted from leakage from damaged hepatocytes (hepatocellular injury). The biomarkers of hepatic function, ALT, AST and GGT, were considered in this study. In this study, mice groups implanted with EAC caused a significant increase in the serum activities of ALT, AST and GGT. ALT and AST are primarily located in the cytoplasm and mitochondria of hepatocytes [10-13]. In this study, treatment with nano- Chl protected against increase in serum levels of ALT, AST, and GGT, which is an indication of hepato-protection by nano-Chl or nano-5-ALA. This also confirms the protective role of nano- Chl against hepato-dysfunction.

Conclusion

It can be concluded that the present study opened new trends for cancer treatment therapy that needs to be further verified. The study gave profound results involving the use of sono-photo-dynamic modality employing exposure to infra-red laser and ultrasound, pulsed and continuous, in combination with nano-Chl or nano-5-ALA as a sono-photo sensitizer for treating Ehrlich Ascites Carcinoma tumor implanted. The possible application of nano-carrier-sono-photo-dynamic therapy as *in vivo* anti-malignancy can open new line of research for modern cancer therapy that needs to be further investigated.

References

1. Carstensen EL, Kelly P, Church CC, Brayman AA, Child SZ, Raeman CH, Schery L. Lysis of erythrocytes by exposure to CW ultrasound. Ultras Med Biol 1993; 19: 147-65.
2. Honda H, Zhao QL, Kondo T. Effects of dissolved gases and an echo contrast agent on apoptosis induced by ultrasound and its mechanism via the mitochondria-caspase pathway. Ultras Med Biol 2002; 28: 673-82.

3. Feril LB, Kondo T, Zhao QL, Ogawa R, Tachibana K, Kudo N, Fujimoto S, Nakamura S. Enhancement of ultrasound-induced apoptosis and cell lysis by echo-contrast agents. Ultras Med Biol 2003; 29: 331-7.
4. Miller MW, Miller DL, Brayman AA. A review of in vitro bioeffects of inertial ultrasonic cavitation from a mechanistic perspective. Ultras Med Biol 1996; 22: 1131-54.
5. Feigl T, Völklein B, Iro H, Ell C, Schneider T. Biophysical effects of high-energy pulsed ultrasound on human cells. Ultras Med Biol 1996; 22: 1267-75.
6. Fry FJ, Goss SA, Patrick JT. Transkull focal lesions in cat brain produced by ultrasound. J Neurosurg1981; 54: 659-63.
7. Kondo T, Kano E. Effect of free radicals induced by ultrasonic cavitation on cell killing. Int J Rad Biol 1988; 54: 475-86.
8. Ashush H, Rozenszajn LA, Blass M, Barda-Saad M, Azimov D, Radnay J, Zipori D, Rosenschein U. Apoptosis induction of human myeloid leukemic cells by ultrasound exposure. Cancer Res 2000; 60: 1014-20.
9. Feril LB, Kondo T. Biological effects of low intensity ultrasound: the mechanism involved, and its implications on therapy and on biosafety of ultrasound. J Rad Res 2004; 45: 479-89.
10. Boone L, Meyer D, Cusick P, Ennulat D, Bolliger AP, Everds N. Selection and interpretation of clinical pathology indicators of hepatic injury in preclinical studies. Vet Clin Pathol 2005; 34:182-8.
11. Singh A, Bhat TK, Sharma OM. Clinical biochemistry of hepatotoxicity. J Clinic Toxicol 2011; 4: 1-19.
12. Ozer J, Ratner M, Shaw M, Bailey W, Schomaker S. The current state of serumbiomarkers of hepatotoxicity. Toxicology 2008; 245: 194-205.
13. Ramaiah S. A toxicologist guide to the diagnostic interpretation of hepatic biochemical parameters. Food ChemToxicol 2007; 45: 1551–7.
14. Amacher D. A toxicologist's guide to biomarkers of hepatic response. Hum Exp Toxicol 2002; 21: 253-62.
15. Han W, Bonventre J. Biologic markers for the early detection of acute kidney injury. Curr Opin Crit Care 2004; 10: 476–82.
16. George G, Wakasi M, Egoro E. Creatinine and urea levels as critical markers in end-stage renal failure. Research and Review: J Med Heal Sci 2014; 3: 41-4.
17. Paliwal R, Sharma V, Pracheta, Sharma S, Yadav S, Sharma SH. Antinephrotoxic effect of administration of Moringaoleifera Lam. in amelioration of DMBA-induced renal carcinogenesis in Swiss albino mice. Biol Med 2011; 3:27-35.
18. Sharma V, Paliwal R, Janmeda P, Sharma SH. The reno-protective efficacy of Moringaoleifera pods on xenobiotic enzymes and antioxidant status against 7,12-dimethylbenz[a]anthracene exposed mice. J Chin Integr Med 2012; 10:1171-8.
19. Johnsson B, Lofas S, Lindquist G. Immobilization of proteins to a carboxymethyldextran-modified gold surface for biospecific interaction analysis in surface plasmon resonance sensors. Anal Biochem 1991; 198: 268-77.
20. Sener D, Gönenç A, Akinci M, Torun M. Lipid peroxidation and total antioxidant status in patients with breast cancer. Cell BiochemFunct 2007; 25: 377-82.
21. Revathi R, Manju V. The effects of Umbelliferone on lipid peroxidation and antioxidant status in diethylnitrosamine induced hepatocellular carcinoma. J Acute Medicine 2013; 3: 73-82.
22. Wu G, Fang YZ, Yang S, Lupton JR, Turner ND. Glutathione metabolism and its implications for health. J Nutr 2004; 134: 489-92.
23. Blair IA. Endogenous glutathione adducts. Curr Drug Metab 2006; 7: 853-72.

24. Kumaraguruparan R, Subapriya R, Kabalimoorthy J, Nagini S. Antioxidant profile in the circulation of patients with fibroadenoma and adenocarcinoma of the breast. Clin Biochem 2002; 35: 275-9.
25. Pradeep K, Mohen CV, Gobian K, Karthikeyan S. Silymarin modulates the oxidant-antioxidant imbalance during diethylnitrosamine induced oxidative stress in rats. Eur J Pharmacol 2007; 560: 110-16.
26. Bishayee K, Ghosh S, Mukherjee A, Sadhukhan R, Mondal JK, Bukhsh AR. Quercetin induces cytochrome-c release and ROS accumulation to promote apoptosis and arrest the cell cycle in G2/ M, in cervical carcinoma: signal cascade and drug–DNA interaction. Cell Prolif 2013; 46:153-63.